

replaced by nitrogen, the solvent was filtered off, and the pink residue was washed with pentane ( $2 \times 5$  mL). The solid was dried in vacuo, during which the color slowly changed from pink to red-brown, dissolved in toluene (20 mL), and subsequently cooled to  $-80$  °C. Workup gave 100 mg (0.22 mmol, 18%) of 20 as red-brown crystals. IR ( $\text{cm}^{-1}$ ): 2710 (w), 2120 (w), 1600 (m), 1030 (m), 940 (m), 800 (w), 730 (w), 450 (m). NMR data are given in Table II. Anal. Calcd for  $\text{C}_{23}\text{H}_{33}\text{Ce}$ : C, 61.44; H, 7.40; Ce, 31.16. Found: C, 61.59; H, 7.34; Ce, 31.25.

**Catalytic Dimerization of *tert*-Butylacetylene by  $[\text{Cp}^*_2\text{CeC}\equiv\text{C}-t\text{-Bu}]_n$  (7).** A 50- $\mu\text{L}$  (0.4 mmol) aliquot of *tert*-butylacetylene was added to an NMR tube containing a suspension of 10.0 mg (0.02 mmol) of 7 in benzene- $d_6$  (0.5 mL). Upon addition the solution turned purple and subsequently red-brown. NMR analysis showed that all *tert*-butylacetylene had selectively been dimerized to 2,4-di-*tert*-butyl-1-buten-3-yne (10).

**Preparation of  $\text{Cp}^*_2\text{CeC}\equiv\text{C}-t\text{-Bu}\cdot\text{THF}$  (8).** *tert*-Butylacetylene (0.1 mL, 0.8 mmol) was added to a stirred solution of

205 mg (0.36 mmol) of  $\text{Cp}^*_2\text{CeCH}(\text{SiMe}_3)_2$  in pentane/THF (11 mL, 10:1). Upon addition the color of the solution changed from red to orange. The solution was evaporated to dryness to remove THF, and the residue was redissolved in pentane (10 mL). Concentration and cooling to  $-80$  °C gave 88 mg (0.16 mmol, 44%) of 8 as orange-red crystals. IR ( $\text{cm}^{-1}$ ): 2725 (w), 2140 (w), 2060 (m), 1360 (m), 1245 (s), 1200 (w), 1020 (s), 865 (m), 715 (m), 480 (m). NMR data are given in Table II. Anal. Calcd for  $\text{C}_{30}\text{H}_{47}\text{CeO}$ : C, 63.91; H, 8.40; Ce, 24.85. Found: C, 63.97; H, 8.47; Ce, 24.76.

**Acknowledgment.** We thank Dr. A. P. Bruins, Mr. E. v. d. Meulen, and Mr. A. Kiewiet for recording the GC/MS spectra and Shell Research B.V. for financial support.

**Supplementary Material Available:** A text section containing the spectroscopic characterization of the alkyne oligomers 9-19 (4 pages). Ordering information is given on any current masthead page.

## A Carbido Cluster as a Bulky $\pi$ Donor Ligand. Preparation and Characterization of $[\text{HFe}_4(\text{CO})_{12}\text{C}]\text{BXY}$ (X = Y = H, Cl, Br; X = H, Y = Cl, Br, OH)

Xiangsheng Meng, Nigam P. Rath, and Thomas P. Fehlner\*

Department of Chemistry and Biochemistry, University of Notre Dame, Notre Dame, Indiana 46556

Arnold L. Rheingold\*

Department of Chemistry and Biochemistry, University of Delaware, Newark, Delaware 19716

Received November 19, 1990

The preparation and characterization of the compounds  $[\text{HFe}_4(\text{CO})_{12}\text{C}]\text{BXY}$  (X = Y = H, Cl, Br; X = H, Y = Cl, Br, OH) are described. Geometric, spectroscopic, and Fenske-Hall quantum-chemical parameters demonstrate that these compounds are usefully described as tricoordinate boron compounds substituted with a carbido cluster. The carbido cluster  $[\text{HFe}_4(\text{CO})_{12}\text{C}]$ , as a substituent, is shown to be both a sterically demanding ligand and a strong  $\pi$  donor to the boron center. The unanticipated differences in the reactivity of these compounds with  $\text{AlX}_3$ ,  $\text{NET}_3$ ,  $\text{H}_2\text{O}$ , and THF as X and Y are varied reflect the unusual properties of this compound type. Single-crystal X-ray diffraction studies of  $[\text{HFe}_4(\text{CO})_{12}\text{C}]\text{BHX}$  (X = Cl, Br) are reported. In both cases crystals form in the monoclinic system of space group  $P2_1/m$  with the following unit cell parameters: X = Cl,  $a = 8.081$  (2) Å,  $b = 15.730$  (3) Å,  $c = 8.936$  (2) Å,  $\beta = 113.41$  (2)°,  $V = 1042.3$  (4) Å<sup>3</sup>,  $Z = 2$ ; X = Br,  $a = 8.276$  (6) Å,  $b = 15.749$  (11) Å,  $c = 8.993$  (6) Å,  $\beta = 114.36$  (6)°,  $V = 1067.7$  (1.5) Å<sup>3</sup>,  $Z = 2$ . The solution for X = Cl was by direct methods ( $R(F) = 3.27\%$ ,  $R(wF) = 3.55$  for 1656 independent reflections ( $F_o > 5\sigma F_o$ )), whereas for X = Br it was by isomorphous analogy to the solution for X = Cl ( $R(F) = 3.97\%$ ,  $R(wF) = 4.11\%$  for 1889 independent reflections ( $F_o > 5\sigma F_o$ )).

The usefulness of boranes as reagents is well-known.<sup>1</sup> Part of this success is due to the fact that a versatile derivative chemistry is known whereby the properties of the boron center can be systematically varied by appropriate steric and electronic factors associated with the substituents at the boron center. The effect of transition-metal fragments as borane substituents on reactivity and properties is less well understood. On the other hand, in those systems that have been studied, the complex M-B interactions are known to change the reactivity of the B-H bond extensively.<sup>2-11</sup> However, until recently there was

no report of a boron hydride substituted with a mononuclear transition-metal fragment, e.g.  $L_2\text{MBH}_2$ . An example from our own laboratories is  $(\text{CO})_4\text{CoBH}_2\cdot\text{THF}$ ,<sup>12</sup> and the closely related complex  $(\text{CO})_2(\eta^1\text{-dppm})\text{Co}(\mu\text{-dppm})\text{BH}_2$  has now been isolated and crystallographically charac-

(4) Schmid, G.; Batzel, V.; Elzrodt, G.; Pfeil, R. *J. Organomet. Chem.* 1975, 86, 257.

(5) Johnson, B. F. G.; Eady, C. R.; Lewis, J. *J. Chem. Soc., Dalton Trans.* 1977, 477.

(6) Housecroft, C. E. *Polyhedron* 1987, 6, 1935. Chipperfield, A. K.; Housecroft, C. E. *J. Organomet. Chem.* 1988, 349, C17.

(7) Baker, R. T. *Abstr. Pap.-Am. Chem. Soc.* 1986, 192nd, INOR 143.

(8) Jensen, J. A.; Wilson, S. R.; Girolami, G. S. *J. Am. Chem. Soc.* 1988, 110, 4977.

(9) Ting, C.; Messerle, L. *J. Am. Chem. Soc.* 1989, 111, 3449.

(10) Fehlner, T. P. *New J. Chem.* 1988, 12, 307.

(11) Schmid, G. *Angew. Chem., Int. Ed. Engl.* 1970, 9, 819. Nöth, H.; Schmid, G. *Allg. Prakt. Chem.* 1966, 17, 610. Nöth, H.; Schmid, G. *J. Organomet. Chem.* 1966, 5, 109. Schmid, G.; Nöth, H. *J. Organomet. Chem.* 1967, 7, 129.

(12) Basil, J. D.; Aradi, A. A.; Bhattacharyya, N. K.; Rath, N. P.; Eigenbrot, C.; Fehlner, T. P. *Inorg. Chem.* 1990, 29, 1260.

(1) Brown, H. C. *Organic Syntheses via Boranes*; Wiley: New York, 1975.

(2) Parshall, G. W. *J. Am. Chem. Soc.* 1964, 86, 361.

(3) Hertz, R. K.; Goetze, R.; Shore, S. G. *Inorg. Chem.* 1979, 18, 2813. Plotkin, J. S.; Shore, S. G. *J. Organomet. Chem.* 1979, 182, C15. Shore, S. G.; Jan, D.-Y.; Hsu, L.-Y.; Hsu, W.-L. *J. Am. Chem. Soc.* 1983, 105, 5923. Shore, S. G.; Jan, D.-Y.; Hsu, W.-L.; Hsu, L.-Y.; Kennedy, S.; Huffman, J. C.; Lin Wang, T.-C.; Marshall, A. J. *Chem. Soc., Chem. Commun.* 1984, 392. Workman, D. P.; Jan, D.-Y.; Shore, S. G. *Inorg. Chem.* 1990, 29, 3518.

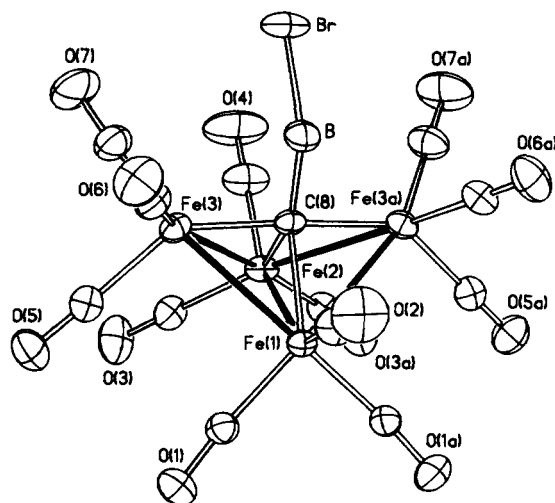


Figure 1. Molecular structure of  $[\text{HFe}_4(\text{CO})_{12}\text{C}]\text{BHBr}$ . The B-H and Fe(1)-H-Fe(2) hydrogen atoms are not shown.

terized by others.<sup>13</sup> Formation of this type of species has also been found to occur via oxidative addition of a B-H bond to a transition metal, e.g.,  $(\text{PMe}_3)_3\text{Ir}(\text{H})_2\text{BR}_2$ <sup>14</sup> and  $(\text{C}_6\text{H}_4\text{O}_2\text{B})\text{Ir}(\text{H})(\text{Cl})(\text{PMe}_3)_3$ , which contains two B-O and one B-Ir bond.<sup>15</sup> Because of the substituents on the boron atom, the monoboron iridium compounds do not have a base coordinated to the boron atom.<sup>15</sup> In all of these compounds the metal-boron interaction is a direct one, i.e., primarily  $\sigma$  in nature. Here we present the synthesis and characterization of a mononuclear borane in which, in addition to the  $\sigma$  interaction with a carbido carbon, the interaction with the metal atoms of the multinuclear transition-metal cluster itself is via a  $\pi$  rather than  $\sigma$  interaction and no additional Lewis base is associated with the boron center.

In the development of a new route to  $\text{HFe}_3(\text{CO})_9\text{BH}_4$ , trace quantities of a new compound were isolated and this species,  $[\text{HFe}_4(\text{CO})_{12}\text{C}]\text{BH}_2$ , was structurally characterized.<sup>16</sup> Because of its unusual geometric features and associated electronic structure, we sought better routes into this system. It had already been demonstrated by Shriver and co-workers that protonation of  $[\text{Fe}_4(\text{CO})_{13}]^{2-}$  with strong acid leads to the formation of the carbido cluster  $\text{HFe}_4(\text{CO})_{12}\text{CH}$ .<sup>17</sup> Further, the known reaction of  $\text{BH}_3 \cdot \text{THF}$  with CO in the presence of hydride to yield trimethylboroxine hints at reasonable pathways for cleaving the C-O bond of a coordinated CO.<sup>18,19</sup> Thus, we speculated that the use of  $\text{BH}_3$  followed by a source of  $[\text{H}]^+$  might lead to  $[\text{HFe}_4(\text{CO})_{12}\text{C}]\text{BH}_2$ .<sup>20</sup> Although the strategy was successful, the modest yields of  $[\text{HFe}_4(\text{CO})_{12}\text{C}]\text{BH}_2$  isolated from this reaction ruled out a mechanistic study. On the other hand, sufficient material was prepared by this route to define more fully the structure and reactivity of this unusual molecular system.

(13) Elliot, D. J.; Levy, C. J.; Puddephatt, R. J.; Holah, D. G.; Hughes, A. N.; Magnuson, V. R.; Moser, I. M. *Inorg. Chem.* 1990, 29, 5014.

(14) Churchill, M. R.; Hackbarth, J. J.; Davison, H.; Traficante, D. D.; Wreford, S. S. *J. Am. Chem. Soc.* 1974, 96, 4041.

(15) Merola, J. S.; Knorr, J. R. *Abstr. Pap.—Am. Chem. Soc.* 1990, 199th, INOR 392.

(16) Meng, X.; Rath, N. P.; Fehlner, T. P. *J. Am. Chem. Soc.* 1989, 111, 3422.

(17) Whitmire, K.; Shriver, D. F. *J. Am. Chem. Soc.* 1980, 102, 1456.

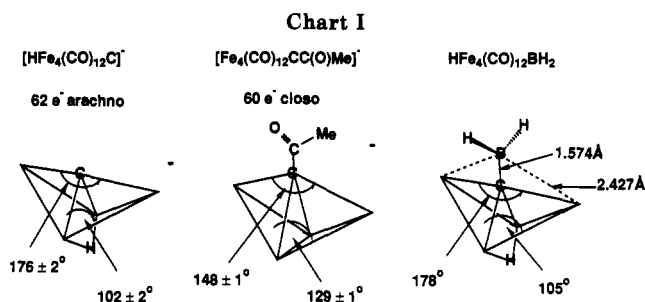
(18) Rathke, M. W.; Brown, H. C. *J. Am. Chem. Soc.* 1966, 88, 2606.

(19) Lavigne, G. In *The Chemistry of Metal Cluster Complexes*; Shriver, D. F., Kaesz, H. D., Adams, R. D., Eds.; VCH: New York, 1990; p 270.

(20) Holt, E. M.; Whitmire, K. H.; Shriver, D. F. *J. Organomet. Chem.* 1981, 213, 125.

Table I. Selected Bond Distances and Angles for  $[\text{HFe}_4(\text{CO})_{12}\text{C}]\text{BH}X$  (X = Cl, Br)

	X = Cl	X = Br
(a) Bond Distances (Å)		
Fe(1)–Fe(2)	2.598 (1)	2.604 (1)
Fe(1)–Fe(3)	2.654 (1)	2.660 (1)
Fe(2)–Fe(3)	2.678 (1)	2.686 (1)
Fe(1)–C(8)	1.954 (4)	1.968 (6)
Fe(2)–C(8)	1.921 (5)	1.921 (8)
Fe(3)–C(8)	1.860 (1)	1.864 (1)
C(8)–B	1.566 (10)	1.551 (13)
B–X	1.826 (6)	1.981 (8)
Fe(3)–B	2.453 (3)	2.446 (3)
(b) Bond Angles (deg)		
Fe(1)–Fe(2)–Fe(3)	60.4 (1)	60.4 (1)
Fe(1)–Fe(3)–Fe(2)	58.3 (1)	58.3 (1)
Fe(1)–C(8)–Fe(3)	88.1 (1)	87.9 (2)
Fe(1)–C(8)–Fe(2)	84.2 (2)	84.1 (3)
Fe(1)–Fe(3)–C(8)	47.4 (1)	47.7 (2)
Fe(1)–Fe(2)–C(8)	48.5 (1)	48.7 (2)
Fe(2)–Fe(1)–Fe(3)	61.3 (1)	61.3 (1)
Fe(2)–C(8)–Fe(3)	90.2 (2)	90.4 (2)
Fe(2)–Fe(1)–C(8)	47.4 (2)	47.2 (2)
Fe(2)–Fe(3)–C(8)	45.8 (2)	45.7 (2)
Fe(3)–Fe(2)–C(8)	44.0 (1)	44.0 (1)
Fe(3)–Fe(1)–C(8)	44.5 (1)	44.5 (1)
Fe(1)–C(8)–B	133.3 (4)	132.2 (5)
Fe(2)–C(8)–B	142.5 (3)	143.7 (4)
Fe(3)–C(8)–B	91.0 (2)	91.0 (2)
C(8)–B–X	122.2 (5)	123.0 (6)
Fe(3)–C(8)–Fe(3a)	176.2 (2)	175.6 (2)

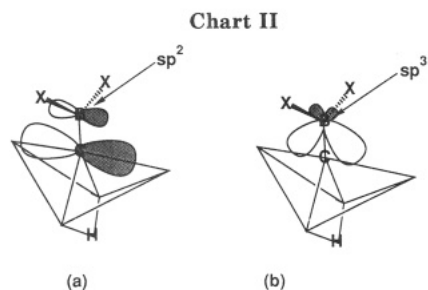


## Results and Discussion

**Solid-State Structures.** The molecular structure of  $[\text{HFe}_4(\text{CO})_{12}\text{C}]\text{BHBr}$  is shown in Figure 1, and selected bond distances and angles for it and the chloro derivative are given in Table I. Both have the same essential structural features of the solid-state structure of  $[\text{HFe}_4(\text{CO})_{12}\text{C}]\text{BH}_2$  communicated earlier.<sup>16</sup> In essence they all are composed of a known carbido cluster fragment,  $[\text{HFe}_4(\text{CO})_{12}\text{C}]$ , bound to a  $[\text{BH}X]$  fragment and it is useful to consider the structures in terms of these fragments. The Fe-Fe distances are similar to those reported in other "saturated"  $\text{Fe}_4\text{C}$  "butterfly" complexes,<sup>21</sup> even though some distortion of the iron cage is noted for the Cl and Br derivatives due, presumably, to the larger radius of the halogens relative to that of H. A key structural factor is the dihedral angle between the "wings" of the butterfly or, alternatively, the wingtip Fe-carbide C-wingtip Fe angle. A 62-electron butterfly exhibits a dihedral angle of  $102 \pm 2^\circ$  and an Fe-C-Fe angle of  $176 \pm 2^\circ$  compared to  $129 \pm 1$  and  $148 \pm 1^\circ$ , respectively, for the 60-electron system.<sup>22</sup>

(21) Beno, M. A.; Williams, J. M.; Tachikawa, M.; Muettterties, E. L. *J. Am. Chem. Soc.* 1981, 103, 1485. Holt, E. M.; Whitmire, K. H.; Shriver, D. F. *J. Organomet. Chem.* 1981, 213, 125. Bradley, J. S.; Ansell, G. B.; Leonowicz, M. E.; Hill, E. W. *J. Am. Chem. Soc.* 1981, 103, 4968. Fjare, D. E.; Gladfelter, W. L. *Inorg. Chem.* 1981, 20, 3532. Sappa, E.; Tiripichio, A.; Carty, A. J.; Toogood, G. E. *Prog. Inorg. Chem.* 1987, 35, 437.

(22) Bradley, J. S.; Harris, S.; Newsam, J. M.; Hill, E. W.; Leta, S.; Modrick, M. A. *Organometallics* 1987, 6, 2060.



Here the dihedral and Fe–C–Fe angles are 105 and 178, 106 and 176, and 106 and 176° for X = H, Cl, and Br, respectively. These data are summarized in Chart I, where it is clear that the geometry of the carbido cluster fragment in  $[\text{HFe}_4(\text{CO})_{12}\text{C}]\text{BX}_2$  is much closer to that of the 62-electron model rather than the 60-electron cluster. The electronic consequences of this observation are discussed below.

The B–H and B–X distances are normal. The H–B–H and C–B–H angles for X = H are 120.1 (2) and 121.8 (3), 118.0 (4)°, respectively, while for X = Cl, Br the C–B–X angles are 122.1 (5) and 123.0 (6)°, respectively, suggesting trigonal nearest-neighbor geometry around the boron atom. The BHX fragment, the carbido carbon, “hinge” iron atoms, the two attached axial CO’s, and, in the case of X = H, the Fe–Fe bridging H are coplanar. Two boron–carbido carbon distances are normal for a B–C single bond (1.574 (6), 1.566 (10), 1.551 (13) Å), as the reported values for single and double bonds are ~1.6 and 1.361 (5) Å, respectively.<sup>23,24</sup> However, the wingtip Fe–B distances are significantly longer than known Fe–B bonding interactions (2.427 (3), 2.453 (3), and 2.446 (3) Å for X = H, Cl, Br, respectively). A normal Fe–B, unbridged bonding distance is ~2.1 Å,<sup>25</sup> and the Fe–B distance in the Fe–H–B bridged interaction in  $\text{Fe}_2(\text{CO})_6\text{B}_3\text{H}_7$  is ~2.3 Å.<sup>26</sup>

These geometric parameters provide an initial look at the cluster bonding. At the level of counting electrons the structure of  $[\text{HFe}_4(\text{CO})_{12}\text{C}]\text{BHX}$  is interesting, as the first possibility that comes to mind is a 62-electron (closo) octahedral cluster with four  $\text{Fe}(\text{CO})_3$ , one CH, and one BH fragment at the six vertices. Such structural types are well-known for both carbon (e.g.,  $\text{Co}_4(\text{CO})_{10}\text{C}_2\text{Et}_2$ )<sup>27</sup> and boron (e.g.,  $\text{H}_2\text{Cp}_4\text{Co}_4\text{B}_2\text{H}_2$ ).<sup>28</sup> In any event, the isomeric structure isolated contains  $[\text{HFe}_4(\text{CO})_{12}\text{C}]$  and  $[\text{BHX}]$  fragments joined by an apparent B–C single bond. This creates a problem from the point of view of electron counting, as the carbidoiron fragment would then be expected to have the same cluster geometry as that found in  $[\text{Fe}_4(\text{CO})_{12}\text{CC}(\text{O})\text{Me}]^-$ , i.e., a geometric structure corresponding to 60 cluster electrons rather than that of 62 electrons as observed.<sup>29</sup> Basically, the problem resides around the fact that, to produce an exo cluster bonding orbital centered on the carbido carbon, the cluster geom-

Table II. Comparison of Spectroscopic and Structural Parameters for  $[\text{HFe}_4(\text{CO})_{12}\text{C}]\text{BXY}$

X, Y	$J_{\text{BH}}$ , Hz	$\nu(\text{BH})$ , $\text{cm}^{-1}$	$\delta(^{11}\text{B})$ , ppm	$\delta(^{13}\text{C})$ , ppm	$\delta(^1\text{H})$ , ppm	$d_{\text{BC}}$ , Å
H, H	90	2530, 2470	9.3	404.3	4.0, -25.85	1.574 (6)
H, Cl	160	2552	21.2	373.1	5.6, -26.60	1.566 (10)
H, Br	134	2550	14.1	373.6	6.0, -26.59	1.551 (13)
Cl, Cl			30.1	342.3	-26.95	<i>b</i>
Br, Br			15.2	<i>b</i>	-26.97	<i>b</i>
H, OH	140	2510	26.3	<i>b</i>	5.5, -26.72	<i>b</i>

<sup>a</sup> Carbido carbon only. <sup>b</sup> Not measured.

etry must distort from that of the *arachno*- $\text{HFe}_4(\text{CO})_{12}\text{CH}$  to that of the *closo*- $[\text{Fe}_4(\text{CO})_{12}\text{CC}(\text{O})\text{Me}]^-$ .<sup>30</sup>

However, the Fe–C edges of a 62-electron  $[\text{HFe}_4(\text{CO})_{12}\text{C}]^-$  fragment are electron-rich and a  $[\text{BHX}]^+$  fragment that is  $\text{sp}^3$ -hybridized could interact with each as indicated in Chart IIb. However, the measured angles around boron suggest a hybridization closer to  $\text{sp}^2$  rather than  $\text{sp}^3$  and the C–B distance must be considered a bonding distance. Hence, the geometric data force one to adopt the model in Chart IIa, in which an  $\text{sp}^2$ -hybridized boron is singly bonded to the carbido carbon atom and the empty 2p orbital on boron interacts strongly with the electron density present in the carbon–wingtip iron edge. For a very strong  $\pi$  interaction the structures shown in Chart II become indistinguishable. Presumably, the  $\pi$  interaction is sufficiently strong to prevent the  $[\text{HFe}_4(\text{CO})_{12}\text{C}]$  cluster from adopting the 60-electron geometry. The spectroscopic data allow this point to be investigated.

**Spectroscopic Parameters.** Additional information on the bonding between the carbido cluster and borane fragment is revealed by the spectroscopic data. These data are presented in a comparative fashion in Table II for  $[\text{HFe}_4(\text{CO})_{12}\text{C}]\text{BXY}$ . For a substituted borane, the magnitudes of the  $J_{\text{BH}}$  coupling constant and the BH stretching frequency are sensitive to the nature of the substituents and a correlation between these two parameters has been observed.<sup>31</sup> For X = Y = H,  $J_{\text{BH}}$  is in the lower range for terminal B–H coupling constants, suggesting that the effective electronegativity of the carbido cluster as a substituent is similar to that of boron. Replacement of one H with Cl, Br, or OH results in a large increase in  $J_{\text{BH}}$ . This is consistent with the substitution of a more electronegative atom which demands more p character in its  $\sigma$  bond, thereby forcing more s character into the remaining B–H bond. The modest increase in the B–H stretching frequency on substitution is consistent with increased s character in the B–H bond. If the B–H bond is forced to pick up greater s character, then the B–C bond should as well. Indeed, both the Cl and Br derivatives have somewhat shorter B–C distances, although the experimental error in the distances is large relative to the shortening on substitution.

If the limiting structure shown in Chart IIa is operational, then a replacement of one or both of the H’s on the boron atom with  $\pi$  donors should also result in competition between the carbido cluster substituent and the H atom replacement for the empty B 2p orbital. Evidence for the existence of a competitive  $\pi$  interaction comes from the changes in the  $^{13}\text{C}$  chemical shift of the carbido carbon atom with halogen substitution. For X = Y = H the chemical shift is similar to that observed for the discrete carbido cluster. Changes in the carbido cluster to boron  $\pi$  back-bonding should perturb the filled and virtual MO’s with high C 2p character because it is the energy and C

(23) Saturnino, D. J.; Yamauchi, M.; Clayton, W. R.; Nelson, W. R.; Shore, S. G. *J. Am. Chem. Soc.* 1975, 97, 6063. Hsu, L.-Y.; Mariategui, J. F.; Niedenzu, K.; Shore, S. G. *Inorg. Chem.* 1987, 26, 143.

(24) Boese, R.; Paetzold, P.; Tapper, A.; Ziembuiski, R. *Chem. Ber.* 1989, 122, 1057.

(25) Wong, K. S.; Scheidt, W. R.; Fehlner, T. P. *J. Am. Chem. Soc.* 1982, 104, 1111. Fehlner, T. P.; Housecroft, C. E.; Scheidt, W. R.; Wong, K. S. *Organometallics* 1983, 2, 825.

(26) Haller, K. J.; Andersen, E. L.; Fehlner, T. P. *Inorg. Chem.* 1981, 20, 309.

(27) See: Fox, J. R.; Gladfelter, W. L.; Geoffroy, G. L.; Tavanaiepour, I.; Abdel-Mequid, S.; Day, V. W. *Inorg. Chem.* 1981, 20, 3230 and references therein.

(28) Feilong, J.; Fehlner, T. P.; Rheingold, A. L. *J. Am. Chem. Soc.* 1987, 109, 1860.

(29) Bradley, J. S.; Ansell, G. B.; Leonowicz, M. E.; Hill, E. W. *J. Am. Chem. Soc.* 1981, 103, 4968.

(30) Harris, S.; Bradley, J. S. *Organometallics* 1984, 3, 1086.

(31) Watanabe, H.; Nagasawa, K. *Inorg. Chem.* 1967, 6, 1068.

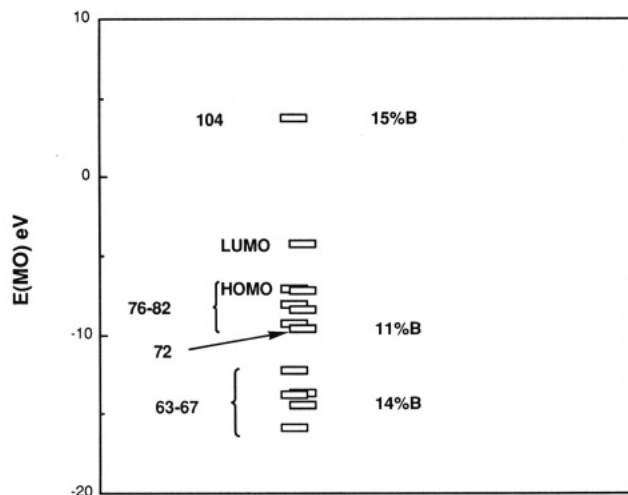


**Figure 2.** Schematic drawing of the eigenvalue spectrum from Fenske-Hall calculations on  $[\text{HFe}_4(\text{CO})_{12}\text{C}]\text{BH}_2$  near the HOMO-LUMO gap. The energies of MO's 84-103 are not shown for clarity. The boron characters of MO's 64, 72, and 104 are indicated.

2p atomic orbital content of these MO's that strongly affect the magnitude of the paramagnetic contribution to the shielding.<sup>32</sup> Thus, substitution of a  $\pi$  donor for H should significantly change the chemical shift of the carbido carbon if competition for the B 2p orbital exists. As shown in Table II, halogen substitution results in an  $\sim 30$  ppm upfield shift per halogen. Although the direction and magnitude of the shift are not predictable without doing actual calculations, the fact that a significant shift is observed is evidence of a significant carbido cluster-boron  $\pi$  interaction.

The  $^{11}\text{B}$  chemical shifts are also consistent with this developing picture of the cluster-boron interaction. The relatively high upfield shift for a formally three-coordinate trigonal boron atom requires the  $[\text{HFe}_4(\text{CO})_{12}\text{C}]$  fragment to function as a  $\pi$ -donating ligand; e.g., the chemical shift of  $\text{BH}_3$  is estimated as  $\sim 57$  ppm, whereas that of  $\text{BF}_3$  is 10 ppm.<sup>33</sup> Greater occupation of the B 2p orbital increases the energy gap between filled and unfilled MO's with high B 2p character, makes the paramagnetic contribution to the shielding less negative, and increases the overall shielding at the  $^{11}\text{B}$  nucleus. In the case of four-coordinate boranes where all three B 2p functions are utilized in bonding and there is no low-lying B 2p orbital, addition of increasingly better  $\pi$ -bonding ligands leads to an increase in the paramagnetic contribution and a decrease in the overall shielding.<sup>19</sup> It will be noted from Table II that replacement of H by Br, Cl, and OH leads to a more and more deshielded boron atom. Hence, one concludes that the boron atom either is effectively four-coordinate or is already using the B 2p orbital in  $\pi$  interactions in  $[\text{HFe}_4(\text{CO})_{12}\text{C}]\text{BH}_2$ . The former does not appear to be consistent with the measured geometric parameters, whereas the latter is essentially the same conclusion forced upon us by the electron-counting considerations discussed above.

**Electronic Structure.** These cluster-borane interactions are revealed in further detail as a result of a Fenske-Hall molecular orbital (MO) treatment of  $[\text{HFe}_4(\text{CO})_{12}\text{C}]\text{BH}_2$ . A schematic diagram of the eigenvalue spectrum near the HOMO-LUMO gap is shown in Figure 2. Most of the MO's are associated with the  $[\text{HFe}_4(\text{CO})_{12}]$

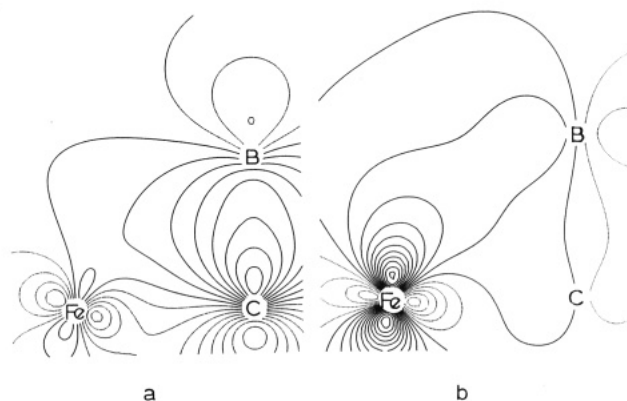


**Figure 3.** Orbital contour diagrams for (a) MO 64 and (b) MO 72 for  $[\text{HFe}_4(\text{CO})_{12}\text{C}]\text{BH}_2$  in a plane containing Fe(3), C(8), and B (see Figure 1). Sixteen values of the function uniformly spaced from  $-0.20$  to  $+0.40$  are plotted for (a) and from  $-0.21$  to  $+0.45$  for (b). MO 64 contains 14% B, 39% C, and 4% Fe(3), whereas MO 72 contains 11% B, 2% C, and 12% Fe(3).

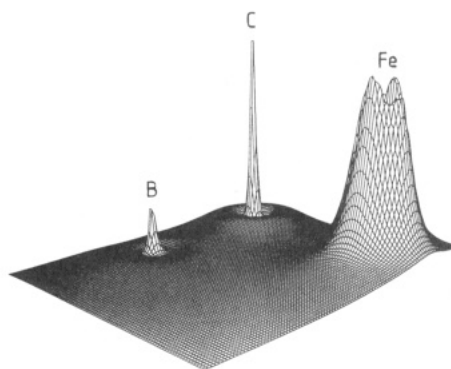


**Figure 4.** Plot of the total electron density for the same atoms and plane described in Figure 3.

fragment, and the electronic structure of this cluster type has been discussed extensively in the past.<sup>34</sup> What is of interest here is the set of MO's that contain both  $[\text{HFe}_4(\text{CO})_{12}]$  fragment and boron atom character. In the filled set these are orbitals 64 and 72 with boron characters indicated in Figure 2 and orbital contours in the vicinity of the carbido carbon, wingtip iron, and boron shown in Figure 3. Clearly MO 64 contains a strong  $\sigma$ -bonding interaction between the carbido carbon and boron atoms, whereas MO 72 corresponds to a weaker, but significant,  $\pi$  (with respect to the C-B axis) interaction between the boron atom and the  $[\text{HFe}_4(\text{CO})_{12}]$  fragment. The plot of the total electron density in the same region, shown in Figure 4, indicates that the primary boron- $[\text{HFe}_4(\text{CO})_{12}]$  fragment interaction does take place via the carbido carbon atom; i.e., the buildup of electron density between the carbon and boron atoms is evident but there is no evidence for the off-axis maximum required by the limiting model in Chart IIb. This substantiates the analysis of the geometric and spectroscopic data presented above. Finally, the Fenske-Hall MO's and energies have been used previously to calculate the relative  $^{11}\text{B}$  chemical shift of  $[\text{HFe}_4(\text{CO})_{12}\text{C}]\text{BH}_2$ .<sup>35</sup> As previously described, the chemical shift correlates well with those calculated for a variety of other molecules containing boron. Simply put, the reason for the relatively shielded tricoordinate boron atom is the fact that the lowest lying empty MO containing

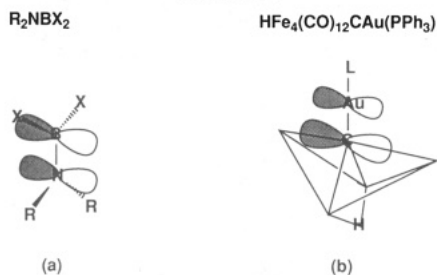
(32) Czech, P. T.; Ye, X.-Q.; Fenske, R. F. *Organometallics* 1990, 9, 2016.

(33) Kidd, R. G. In *NMR of Newly Accessible Nuclei*; Laszlo, P., Ed.; Academic: New York, 1983; Vol. 2, p 49.

(34) See: Harris, S.; Blohm, M. L.; Gladfelter, W. L. *Inorg. Chem.* 1989, 28, 2290 and references therein.

(35) Fehlner, T. P.; Czech, P. T.; Fenske, R. F. *Inorg. Chem.* 1990, 29, 3103.

Chart III



significant B 2p character is MO 104 (Figure 2), which lies considerably above the LUMO. This can be contrasted with the situation of a tricoordinate boron compound with no  $\pi$  interactions in which the LUMO is the low-lying, empty, out-of-plane B 2p atomic orbital.

Hence, we conclude that the overall boron-cluster interaction in  $[HFe_4(CO)_{12}C]BH_2$  is not unlike that in aminoboranes, where, as shown in Chart IIIa, the filled orbital based on the nitrogen atom interacts with the empty orbital on the boron atom. Further,  $[HFe_4(CO)_{12}C]BH_2$  is structurally very similar to  $[HFe_4(CO)_{12}C]Au(PPh_3)^{36}$  (Chart IIIb) with  $[BH_2]^+$  formally replacing the  $[Au(PPh_3)]^+$  fragment. The latter fragment is usually considered a pure  $\sigma$  acceptor analogous to  $[H]^+$ ; however, in this compound it appears to be acting as a  $\pi$  acceptor as well.

**Reactivity.** It is, of course, in reactivity that one finds the expression of geometric and electronic structure, and we have examined selected reactions of  $[HFe_4(CO)_{12}C]BXY$ .

The reaction of  $[HFe_4(CO)_{12}C]BXY$  with Lewis bases is of importance, as one is dealing with a tricoordinate boron center. If the conclusions derived from the structural and spectroscopic data are correct, then both the bulky nature of the cluster ligand and its back-donating ability should inhibit base coordination. With  $NEt_3$  and THF as bases, in no case was an adduct observed. However, this does not eliminate adduct formation, as other reactions were observed. As the reactions with these two bases were different, they are discussed separately. For  $X = H, Y = Cl, Br, OH$  and  $X = Y = Cl, Br$ , reaction with  $NEt_3$  resulted in deprotonation, although it was not a clean reaction for  $X = H, Y = Br$ . The infrared spectrum exhibits a 50–60- $cm^{-1}$  shift of the CO bands to lower energy in the IR spectrum, loss of the  $^1H$  NMR resonance of the metal hydride, and a shift in the  $^{11}B$  NMR resonance with no change in multiplicity. The spectroscopic information clearly indicates that the reaction of  $[HFe_4(CO)_{12}C]BXY$  with triethylamine takes place at the cluster framework and involves deprotonation of the Fe–H–Fe bridge to form the salt  $[NEt_3H][[HFe_4(CO)_{12}C]BXY]$ . This type of behavior is well documented for metal cluster hydrides.<sup>37</sup> In the case of  $X = Y = H$ , reaction with  $NEt_3$  led to decomposition of the complex. Deprotonation probably takes place but, in the absence of a halogen substituent, the B–H bonds become sufficiently hydridic to attack the carbonyl carbon atoms, thereby leading to cluster decomposition.

The reaction of  $[HFe_4(CO)_{12}C]BXY$  with THF is exceedingly complex. For  $X = Y = Cl, Br$  deprotonation takes place to form the same monoanions produced above with  $NEt_3$ . The reaction is reversible in that removal of THF under vacuum followed by addition and removal of

toluene under vacuum results in a product soluble in hexane with the spectroscopic signature of  $[HFe_4(CO)_{12}C]BXY$ . However, in the case of the bromo derivative, the IR spectra indicate the deprotonation reaction is not clean. For  $X = H, Y = OH$ , no reaction occurs with THF. For  $X = Y = H$ , loss of the boron signal in the  $^{11}B$  NMR spectrum is observed and the IR spectrum shows the formation of an unidentified metal carbonyl. The reaction for  $X = H, Y = Cl, Br$  is the most interesting. The spectroscopic evidence shows deprotonation taking place; however, within 30 min additional products are formed. This reaction proceeds to the greatest extent for  $Y = Br$ , in which case  $[HFe_4(CO)_{12}C]BBR_2$  and  $[HFe_4(CO)_{12}C]BH-OH$  are two of at least three products formed, with the hydroxyl derivative being formed in significantly higher yield.

We are not sure of the origin of the oxygen atom in the  $Y = OH$  product. Adventitious  $H_2O$  is an obvious choice, even though the THF was rigorously dried with no apparent effect on the  $Y = OH$  product yield. A more chemically pleasing source is THF, and indeed, it is well-known that the THF ring can be opened by a hydrogen halide to form either a halo alcohol or a dihaloalkane<sup>38</sup> or by halogen to form halide.<sup>39</sup> The initial step in our case may be similar. As the cleavage of THF by  $HX$  increases in the order  $HCl < HBr < HI$ , this may explain why the reaction with  $Y = Br$  is much better than that with  $Cl$  in producing this product. It is interesting to note that borane, chloroborane, and dichloroborane do not react with THF (or do so very slowly).<sup>40</sup> Further, the reactivities of  $BH_2X$  or  $BHX_2$  ( $X = H, Cl, Br$ ) with THF increase in the order  $H < Cl < Br$ .<sup>37</sup> The cluster-substituted borane  $[HFe_4(CO)_{12}C]BHY$  ( $Y = Cl, Br$ ) reacts with THF in the same relative order, but more rapidly than  $BH_2X$  and  $BHX_2$ . Note that the presence of hydride on boron is important, as neither  $BY_3$  nor  $[HFe_4(CO)_{12}C]BY_2$  ( $Y = Cl, Br$ ) cleave THF. The promotion of apparent THF cleavage by the carbido-substituted cluster is consistent with the observation that  $(CO)_4CoBH_2$  cleaves THF much more effectively than  $BH_3$ .<sup>12</sup> Finally, it is appropriate to remember that none of the  $[HFe_4(CO)_{12}C]BXY$  compounds characterized here react with  $H_2O$ .

Hydride replacement on  $[HFe_4(CO)_{12}C]BH_2$  can be carried out with  $AlY_3$  ( $Y = Cl, Br$ ) as the sole halogenation agent. With a mole ratio of  $AlY_3$  to complex of  $\leq 2$  the monosubstituted  $[HFe_4(CO)_{12}C]BHY$  derivative is formed, while with an excess of  $AlY_3$  the disubstituted  $[HFe_4(CO)_{12}C]BY_2$  derivative is formed in quantitative yield. There is little evidence for the direct halogenation of a B–H bond by  $AlX_3$  in the literature. Normally such exchange reactions occur in a direction leading to bond formation between the most electropositive and electronegative elements. This suggests that the boron atom in  $[HFe_4(CO)_{12}C]BH$  is effectively a more electropositive center than the aluminum atom in  $AlY_2$ . However, the halogen exchange reaction of  $AlCl_3$  with 1- $BrB_5H_8$  to yield 2- $ClB_5H_8$  under rather forcing conditions has been reported<sup>41</sup> and  $AlCl_3$  has been used to induce substitution at B–H fragments in metallacarboranes.<sup>42</sup> In the latter case, the proximity of the B–H fragment to the electron-

(38) Haines, A. H. In *Comprehensive Organometallic Chemistry*; Stoddart, J. F., Ed.; Pergamon: Oxford, U.K., 1979; Vol. 1, p 878.

(39) Buchler, C. A.; Pearson, D. E. *Survey of Organic Syntheses*; Wiley: New York, 1970; p 343.

(40) Pasto, D. J.; Balasubramanian, P. *J. Am. Chem. Soc.* **1967**, *89*, 295.

(41) Onak, T.; Dunks, G. B. *Inorg. Chem.* **1964**, *3*, 1060.

(42) Plešek, J.; Heřmánek, S. *Collect. Czech. Chem. Commun.* **1978**, *43*, 1325.

(36) Johnson, B. F. G.; Kaner, D. A.; Lewis, J.; Raithby, P. R.; Rosales, M. J. *J. Organomet. Chem.* **1982**, *231*, C59.

(37) Johnson, B. F. G., Ed. *Transition Metal Clusters*; Wiley: New York, 1975.

rich metal center is thought to be important.

### Conclusions

Metal clusters are not usually viewed as substituents to a main-group center but rather as the center to which other main-group ligands are bound. The geometric and electronic structures of  $[\text{HFe}_4(\text{CO})_{12}\text{C}]\text{BXY}$  illustrate the potential utility of viewing the bulky, electron-rich cluster with high electron mobility as an unusual substituent. The initial studies of the reactivity of these compounds illustrate and support this view. It remains to be seen whether this cluster substituent has sufficient stability under a variety of reaction conditions to be generally useful and whether other clusters can be used as substituents, thereby creating even more unusual chemistry at main-group centers.

### Experimental Section

**General Considerations.** All manipulations were carried out under a nitrogen atmosphere or in a vacuum line by using Schlenk techniques. Solvents were degassed, dried, and distilled before use. Deuterated solvents were dried before use. Products were separated by fractional crystallization or by variable temperature (+20 to -30 °C) column chromatography on 70–230 mesh silica gel 60 (EM Science). The silica gel was dried in an oven overnight before use. Air contained in the silica gel in the column is removed under reduced pressure with use of the vacuum line. Solvent is then added into the column under a nitrogen atmosphere. The bubbles in the column can be removed by pumping (the solvent level must be higher, about 6 cm, than that of silica gel before pumping) until the solvent and the silica gel are well mixed, followed by refilling the column with nitrogen. This process usually removes all bubbles in the column but can be repeated if necessary.

Infrared spectra were recorded on a Perkin-Elmer 1420 spectrometer, and quantitative IR analyses were run on an IBM Model IR32FT-IR instrument using 0.2-mm  $\text{CaF}_2$  solution cells.  $^1\text{H}$  NMR spectra were obtained on Nicolet 300 and GN 300 NMR machines operating at 300 MHz.  $^{13}\text{C}$  NMR spectra were run on a GN 300 spectrometer performing at 75 MHz.  $^{11}\text{B}$  NMR spectra were obtained on a Nicolet 300 spectrometer running at 96 MHz.  $\text{B}_3\text{H}_3\text{N}(\text{Me})_4$  ( $\delta = -29.7$  ppm) was used as an internal reference for  $^{11}\text{B}$  NMR spectra. Chemical shifts for  $^1\text{H}$  and  $^{13}\text{C}$  NMR spectra are recorded in units of  $\delta$  relative to the chemical shifts of deuterated solvents used. Mass spectroscopic characterization was carried out on a Finnigan MAT-8450 spectrometer. The following reagents were used as received without further purification unless otherwise mentioned (Aldrich Chemical Co.):  $\text{Fe}_2(\text{CO})_9$ ,  $\text{AlCl}_3$ ,  $\text{AlBr}_3$ ,  $\text{CCl}_3\text{COOH}$ ,  $\text{CF}_3\text{COOH}$ ,  $\text{Et}_3\text{N}$ ,  $\text{BH}_3\cdot\text{S}(\text{CH}_3)_2$  (2.0 M in toluene or 10.0 M solution),  $\text{BH}_3\cdot\text{THF}$  (1.0 M in THF),  $\text{BH}_2\cdot\text{Cl}\cdot\text{S}(\text{CH}_3)_2$  (9 M),  $\text{BHCl}_2\cdot\text{S}(\text{CH}_3)_2$  (9 M),  $\text{BH}_2\text{Br}\cdot\text{S}(\text{CH}_3)_2$  (1.0 M in dichloromethane or 9.38 M),  $\text{LiC}_4\text{H}_9$  (1.6 M in hexane).

**Synthesis of  $[\text{HFe}_4(\text{CO})_{12}\text{C}]\text{BH}_2$ .** **Method a.** I was first prepared from the reaction of  $\text{Fe}_2(\text{CO})_9$  with  $\text{BH}_3\cdot\text{THF}$  in THF at 55 °C for 3 h.<sup>16</sup>  $\text{Fe}_2(\text{CO})_9$  (5 mmol) was transferred to a 250-mL round-bottom flask. THF (20 mL) was added into the flask. The flask was put into a 50 °C bath, and then 20 mL of  $\text{BH}_3\cdot\text{THF}$  (20 mmol) was added. The reaction was allowed to run 3 h, followed by solvent removal under reduced pressure at 55 °C. After that the flask was taken from the bath, and 5 mL of hexane plus 5 mL of saturated  $\text{CCl}_3\text{COOH}$  in hexane were added to the flask. After the solution was stirred for 30 min, the hexane solution was passed through a low-temperature silica gel column (-15 °C). A tail of the second band (dark red) was collected by using degassed hexane to elute the column. After fractional crystallization in ~80/20 hexane/toluene solution at low temperature, black squarelike crystals were obtained in low yield.

**Method b.** A double-neck, round-bottom, 250-mL flask containing a magnetic stirring bar was fitted with a water-cooled reflux condenser, which was connected to a vacuum line and nitrogen source. A 2-g sample of  $[\text{Fe}(\text{py})_6][\text{Fe}_4(\text{CO})_{13}]^{43}$  was introduced

into the flask via a bent connecting adapter with two inner joints. Toluene (40 mL) then was added.  $\text{BH}_3\cdot\text{SMe}_2$  was added, such that a 3.5:1 ratio of B:Fe was achieved, after the reaction flask had been immersed in a 75 °C oil bath. The reaction was carried out at 75 °C for 3 h, after which toluene was removed under reduced pressure at the reaction temperature until only dark red oily materials remained in the flask. Hexane (20 mL) was added into the flask, and this was followed by 3.5 mL of  $\text{CF}_3\text{COOH}$  added slowly during stirring. The hexane solution changed from colorless to brown. The solution was vigorously stirred for 1 h. After this period the brown solution was transferred into a second flask for the separation of the products. A second, and sometimes a third, 10-mL aliquot of hexane was added to dissolve as much as possible of the products. No more acid was needed. The mixture was passed through a low-temperature silica gel column (-15 °C). The third band (yellow-brown) is the product  $[\text{HFe}_4(\text{CO})_{12}\text{C}]\text{BH}_2$ , and it was collected with use of degassed hexane to elute the column (first two bands: yellow,  $\text{HFe}_3(\text{CO})_9\text{CCH}_3$ ; orange-red,  $\text{HFe}_3(\text{CO})_9\text{BH}_4$ ). After the solution collected was concentrated until saturated, it was then kept in the refrigerator overnight. The pure, crystalline  $[\text{HFe}_4(\text{CO})_{12}\text{C}]\text{BH}_2$  was obtained in about 10% yield.

**Method c.** This reaction was carried out as in method b except that  $[\text{PPN}]_2[\text{Fe}_4(\text{CO})_{13}]^{43}$  rather than  $[\text{Fe}(\text{py})_6][\text{Fe}_4(\text{CO})_{13}]$  was used.  $[\text{HFe}_4(\text{CO})_{12}\text{C}]\text{BH}_2$  was formed in about 15% yield. IR (hexane,  $\text{cm}^{-1}$ ): 2530 w, 2470 w ( $\text{BH}_2$ ); 2055 vs, 2037 vs, 2025 s, 2002 m (CO).  $^{11}\text{B}$  NMR (hexane, 20 °C,  $\delta$ ): 9.75 (br t, fwhm 360 Hz,  $^1\text{H}$ ) 170 Hz;  $J_{\text{B-H}} \approx 90$  Hz).  $^1\text{H}$  NMR ( $\text{C}_6\text{D}_6$ , 20 °C,  $\delta$ ): 4.0 (br s, 2 H), -25.85 (s, 1 H).  $^1\text{H}$  MMR ( $\text{CD}_2\text{Cl}_2$ , 20 °C,  $\delta$ ): 3.9 (br s, 2 H), -25.85 (s, 1 H).  $^{13}\text{C}$  NMR ( $\text{CD}_2\text{Cl}_2$ , 20 °C,  $\delta$ ): 404.35 (s, carbido C), 210.3, 208.48 (s, 12 CO). MS (EI,  $m/e$ ):  $P^+ = 586$  (-12 CO);  $^{56}\text{Fe}_4^{12}\text{C}_{12}^{16}\text{O}_{11}^{11}\text{B}^+\text{H}_3^+$ , 557.714 (obsd), 557.717 (calcd).

**Synthesis of  $[\text{HFe}_4(\text{CO})_{12}\text{C}]\text{BHCl}$ .** The reaction was carried out in the same manner as the preparation of  $[\text{HFe}_4(\text{CO})_{12}\text{C}]\text{BH}_2$  (method b) except that  $\text{BH}_2\text{Cl}\cdot\text{SMe}_2$  was used with a ratio of Fe:B = 1:6. The product  $[\text{HFe}_4(\text{CO})_{12}\text{C}]\text{BHCl}$  was separated from other compounds in the reaction mixture with a cold column (-10 °C). With hexane, the first band (yellow) is  $\text{HFe}_3(\text{CO})_9\text{CCH}_3$ , the second band (brown) is  $[\text{HFe}_4(\text{CO})_{12}\text{C}]\text{BH}_2$  (5%), and the third band (green) is  $[\text{Fe}_3(\text{CO})_{12}]$ .  $[\text{HFe}_4(\text{CO})_{12}\text{C}]\text{BHCl}$  (brown) was collected with use of 50% toluene/50% hexane in about 8% yield. (Note that because of the low solubility of this compound in hexane, three to five hexane extractions during acidification improves the yield significantly.) IR ( $\text{CH}_2\text{Cl}_2$ ,  $\text{cm}^{-1}$ ): 2552 w (BH); 2102 w, 2060 vs, 2043 vs, 2030 s, 2005 m (sh), 2000 m (sh). IR (hexane,  $\text{cm}^{-1}$ ): 2055 vs, 2041 vs, 2028 s, 2008 m, 2001 m (CO).  $^{11}\text{B}$  NMR (hexane, 20 °C,  $\delta$ ): 21.21 (d,  $J_{\text{B-H}} = 160$  Hz).  $^1\text{H}$  NMR ( $\text{CD}_2\text{Cl}_2$ , 20 °C,  $\delta$ ): 5.6 (br s, 1 H), -26.60 (s, 1 H).  $^{13}\text{C}$  NMR ( $\text{CD}_2\text{Cl}_2$ , 20 °C,  $\delta$ ): 373.11 (s, carbido C), 207.60–212.67 (m, 12 CO). MS (EI,  $m/e$ ):  $P^+ = 620$  (-12 CO);  $^{56}\text{Fe}_4^{12}\text{C}_{13}^{16}\text{O}_{12}^{11}\text{B}^{30}\text{Cl}^+\text{H}_2^+$ , 619.6736 (obsd), 619.6731 (calcd).

**Deprotonation of  $[\text{HFe}_4(\text{CO})_{12}\text{C}]\text{BHCl}$ .** A 0.1-mmol amount of the compound in hexane was transferred into a Schlenk flask.  $\text{Et}_3\text{N}$  (0.1 mL) was added drop by drop to the flask with stirring, and brown precipitates were formed. After 30 min the hexane was removed under reduced pressure, leaving the anion  $[\text{Et}_3\text{NH}][\text{Fe}_4(\text{CO})_{12}\text{CBHCl}]$  as a precipitate in the flask. IR (THF,  $\text{cm}^{-1}$ ): 2030 s, 2000 vs, 1965 m, 1940 m.  $^{11}\text{B}$  NMR (THF, 20 °C,  $\delta$ ): 17.0 (d,  $J_{\text{B-H}} \approx 160$  Hz).  $^1\text{H}$  NMR (THF- $d_6$ , 20 °C,  $\delta$ ): 3.26 (br s,  $\text{CH}_2$ ), 1.36 (br s,  $\text{CH}_3$ ).

**Synthesis of  $[\text{HFe}_4(\text{CO})_{12}\text{C}]\text{BHBr}$ .** This compound was prepared with use of the same procedure as that for  $[\text{HFe}_4(\text{CO})_{12}\text{C}]\text{BH}_2$  (method b). Here  $\text{BH}_2\text{Br}\cdot\text{SMe}_2$  was used as the boron source. Again the product  $[\text{HFe}_4(\text{CO})_{12}\text{C}]\text{BHBr}$  is the third band (brown) in the cold column (-20 °C) and can be collected with use of a mixture of hexane and toluene (80/20) after first two bands are washed out with hexane. The cluster can be easily crystallized from hexane solution as needlelike black crystals. The yield of the cluster is about 5%. IR ( $\text{CH}_2\text{Cl}_2$ ,  $\text{cm}^{-1}$ ): 2550 w (BH); 2105 vw, 2060 vs, 2045 s, 2030 s, 2015 m (sh), 2010 m (sh) IR (hexane,  $\text{cm}^{-1}$ ): 2102 vw, 2060 vs, 2045 s, 2032 s, 2015 w, 2010 m.  $^{11}\text{B}$  NMR (hexane, 20 °C,  $\delta$ ): 14.2 (d,  $J_{\text{B-H}} = 134$  Hz).  $^1\text{H}$  NMR ( $\text{CD}_2\text{Cl}_2$ , 20 °C,  $\delta$ ): 6.0 (br s, 1 H), -26.59 (s, 1 H).  $^{13}\text{C}$  NMR ( $\text{CD}_2\text{Cl}_2$ , 20 °C,  $\delta$ ): 373.6 (s, carbido C), 207.6 (s, 12 CO). MS (EI,  $m/e$ ):  $P^+ = 664$  (-12 CO);  $^{56}\text{Fe}_4^{12}\text{C}_{13}^{16}\text{O}_{12}^{11}\text{B}^{80}\text{Br}^+\text{H}_2^+$ .

**Deprotonation of  $[\text{HFe}_4(\text{CO})_{12}\text{C}]\text{BHBr}$ .** By the same procedure as for the deprotonation of  $[\text{HFe}_4(\text{CO})_{12}\text{C}]\text{BHCl}$ , the re-

(43) Whitmire, K. H.; Ross, J.; Cooper, C. B.; Shriver, D. F. *Inorg. Synth.* 1982, 21, 66.

Table III. Crystallographic Parameters for  $C_{13}H_2BClO_{12}Fe_4$  and  $C_{13}H_2BBR_{12}Fe_4$ 

	Y = Cl	Y = Br
(a) Crystal Parameters		
formula	$C_{13}H_2BClO_{12}Fe_4$	$C_{13}H_2BBR_{12}Fe_4$
space group	$P2_1/m$	$P2_1/m$
cryst syst	monoclinic	monoclinic
a, Å	8.081 (2)	8.276 (6)
b, Å	15.730 (3)	15.749 (11)
c, Å	8.936 (2)	8.993 (6)
$\beta$ , deg	113.41 (2)	114.36 (6)
V, Å <sup>3</sup>	1042.3 (4)	1067.7 (1.5)
Z	2	2
cryst dimens, mm	0.48 × 0.38 × 0.38	0.18 × 0.18 × 0.36
cryst color	black	black
D(calc), g/cm <sup>3</sup>	1.975	2.066
$\mu$ (Mo K $\alpha$ ), cm <sup>-1</sup>	29.16	45.75
temp, °C	23	23
T(max)/T(min)	1.585	1.463
(b) Data Collection		
diffractometer	Nicolet R3m	
monochromator	graphite	
scan technique	Wyckoff	
radiation	Mo K $\alpha$ ( $\lambda = 0.71073$ Å)	
2 $\theta$ scan range, deg	4–50	4–52
data collected (hkl)	$\pm 10, +19, +11$	$\pm 11, +20, +12$
no. of rflns collected	2271	2315
no. of indpt rflns	2127	2201
R(merg), %	5.06	4.39
no. of indpt rflns obsd, $F_o \geq 5\sigma(F_o)$	1656	1889
no. of std rflns	3 std/197 rflns	3 std/197 rflns
var in stds, %	<2	<2
(c) Refinement		
R(F), %	3.27	3.97
R(wF), %	3.55	4.11
$\Delta/\sigma$ (max)	0.005	0.002
$\Delta(\rho)$ , e Å <sup>-3</sup>	0.583	0.697
$N_o/N_v$	10.3	10.6
GOF	1.036	1.102

action of  $Et_3N$  with  $[HFe_4(CO)_{12}C]BHBr$  in hexane produces a monoanionic compound. However, in this case other products are also produced, e.g.,  $[HFe_4(CO)_{12}C]B(H)OH$ . <sup>11</sup>B NMR (20 °C, toluene,  $\delta$ ): 12.87 (br, fwhm 120 Hz). <sup>1</sup>H NMR (THF-*d*<sub>6</sub>, 20 °C,  $\delta$ ): 8.1 (br,  $Et_3NH$ ), 5.3 (br, BH), 3.58, 3.19, 1.29 ( $Et_3N$ ).

**Synthesis of  $[HFe_4(CO)_{12}C]B(Cl)_2$ .** Method a. A 0.2-mmol amount of  $[HFe_4(CO)_{12}C]BHCl$  in 10 mL of toluene was introduced into a Schlenk flask containing an excess of  $AlCl_3$  and a magnetic stirring bar. They were combined in a 80 °C oil bath for 3 h. After the mixture was cooled to room temperature, 10 mL of degassed distilled water was added to dissolve the excess unreacted  $AlCl_3$  in the flask. The water was removed by transfer needle. Two or more 10-mL aliquots of degassed water were needed in order to remove all the  $AlCl_3$  from the product  $[HFe_4(CO)_{12}C]B(Cl)_2$ . This compound can be easily crystallized from both hexane and toluene solutions as black crystals.

**Method b.**  $[HFe_4(CO)_{12}C]B(Cl)_2$  can also be formed quantitatively from the reaction of  $[HFe_4(CO)_{12}C]BH_2$  with an excess of  $AlCl_3$  by the procedure described immediately above. IR (hexane, cm<sup>-1</sup>): 2100 w, 2055 vs, 2040 vs, 2027 vs, 2008 s. <sup>11</sup>B NMR (toluene, 20 °C,  $\delta$ ): 30.1 (s). <sup>1</sup>H NMR ( $CD_2Cl_2$ , 20 °C,  $\delta$ ): -26.95 (s, 1 H). <sup>13</sup>C NMR ( $CD_2Cl_2$ , 20 °C,  $\delta$ ): 342.3 (s, carbido C), 207.1, 208.7 (s, 12 CO). MS (EI, m/e):  $P^+ = 654$  (-12 CO); <sup>56</sup>Fe<sub>4</sub><sup>12</sup>C<sub>13</sub><sup>16</sup>O<sub>12</sub><sup>11</sup>B<sup>35</sup>Cl<sub>2</sub><sup>1</sup>H<sup>+</sup>.

**Synthesis of  $[HFe_4(CO)_{12}C]BBR_2$ .** As with  $[HFe_4(CO)_{12}C]B(Cl)_2$ , the title compound was formed quantitatively from the compound  $[HFe_4(CO)_{12}C]BHBr$  or  $[HFe_4(CO)_{12}C]BH_2$  with  $AlBr_3$ . The black crystals crystallize without difficulty from both hexane and toluene solutions. IR (hexane, cm<sup>-1</sup>): 2060 vs, 2042 s, 2030 s, 2015 m (sh), 2008 m. <sup>11</sup>B NMR (toluene, 20 °C,  $\delta$ ): 15.2 (s). <sup>1</sup>H NMR ( $CD_2Cl_2$ , 20 °C,  $\delta$ ): -26.97 (s, 1 H). MS (EI, m/e):  $P^+ = 744$  (-12 CO); <sup>56</sup>Fe<sub>4</sub><sup>12</sup>C<sub>13</sub><sup>16</sup>O<sub>12</sub><sup>11</sup>B<sup>80</sup>Br<sub>2</sub><sup>1</sup>H<sup>+</sup>.

**Deprotonation of  $[HFe_4(CO)_{12}C]BX_2$  (X = Cl, Br).**  $Et_3N$  (0.1 mL) was added drop by drop into a Schlenk flask containing 0.1 mmol of the title compounds in 20 mL of hexane while the

Table IV. Atomic Coordinates ( $\times 10^4$ ) and Isotropic Thermal Parameters ( $\text{Å}^2 \times 10^3$ ) for  $[HFe_4(CO)_{12}C]BHCl$ 

	x	y	z	U <sup>a</sup>
Fe(1)	9501.9 (9)	2500	4343.1 (8)	30.6 (2)
Fe(2)	7615.3 (9)	2500	1215.6 (8)	36.7 (3)
Fe(3)	6984.7 (7)	1318.1 (3)	3082.3 (6)	36.9 (2)
Cl	2916 (2)	2500	1902 (2)	64 (1)
Cl'	5315 (27)	2500	5383 (28)	58 (9)
B	5212 (9)	2500	3466 (8)	45 (2)
O(1)	12318 (4)	1183 (2)	5205 (4)	70 (1)
O(2)	9270 (8)	2500	7533 (5)	90 (3)
O(3)	8985 (6)	1107 (2)	-206 (4)	80 (2)
O(4)	4038 (7)	2500	-1473 (6)	119 (3)
O(5)	9322 (4)	-71 (2)	2839 (4)	67 (1)
O(6)	6614 (5)	633 (2)	6003 (4)	70 (2)
O(7)	3716 (5)	519 (3)	680 (5)	99 (2)
C(1)	11188 (5)	1667 (2)	4857 (5)	44 (1)
C(2)	9341 (8)	2500	6306 (7)	50 (2)
C(3)	8444 (6)	1627 (3)	340 (4)	50 (2)
C(4)	5405 (9)	2500	-385 (7)	67 (3)
C(5)	8439 (5)	466 (2)	2936 (4)	48 (2)
C(6)	6775 (5)	891 (3)	4885 (5)	49 (2)
C(7)	4978 (6)	825 (3)	1609 (5)	59 (2)
C(8)	6907 (6)	2500	3029 (5)	31 (2)

<sup>a</sup> Equivalent isotropic U defined as one-third of the trace of the orthogonalized  $U_{ij}$  tensor.

Table V. Atomic Coordinates ( $\times 10^4$ ) and Isotropic Thermal Parameters ( $\text{Å}^2 \times 10^3$ ) for  $[HFe_4(CO)_{12}C]BHBr$ 

	x	y	z	U <sup>a</sup>
Fe(1)	9491 (1)	2500	4351 (1)	31 (1)
Fe(2)	7582 (1)	2500	1213 (1)	39 (1)
Fe(3)	7001 (1)	1317 (1)	3088 (1)	39 (1)
Br	2813 (1)	2500	1841 (1)	74 (1)
B	5305 (11)	2500	3485 (11)	48 (4)
O(1)	12271 (5)	1193 (2)	5230 (6)	72 (2)
O(2)	9301 (10)	2500	7534 (7)	85 (3)
O(3)	8861 (7)	1106 (3)	-230 (5)	81 (2)
O(4)	4039 (9)	2500	-1507 (9)	124 (4)
O(5)	9320 (5)	-55 (3)	2860 (5)	68 (2)
O(6)	6643 (6)	626 (3)	5994 (5)	75 (2)
O(7)	3771 (6)	496 (4)	674 (7)	106 (3)
C(1)	11150 (6)	1668 (3)	4867 (6)	43 (2)
C(2)	9363 (11)	2500	6296 (9)	52 (3)
C(3)	8365 (7)	1630 (4)	327 (6)	50 (2)
C(4)	5384 (11)	2500	-416 (10)	72 (4)
C(5)	8431 (7)	474 (3)	2939 (6)	47 (2)
C(6)	6801 (7)	881 (3)	4888 (7)	51 (2)
C(7)	5034 (8)	816 (4)	1618 (8)	65 (3)
C(8)	6914 (8)	2500	3021 (8)	34 (2)

<sup>a</sup> Equivalent isotropic U defined as one-third of the trace of the orthogonalized  $U_{ij}$  tensor.

solution was stirred. Brown precipitates formed immediately. After it was stirred about 30 min, the solution became colorless and was removed with a transfer needle. Then the remaining precipitates in the flask were dissolved in THF for spectroscopic examination. X = Cl: IR (THF, cm<sup>-1</sup>) 2030 s, 2000 vs, 1980 m (sh), 1945 m; <sup>11</sup>B NMR (THF, 20 °C,  $\delta$ ) 29.9 (br s); <sup>1</sup>H NMR (THF-*d*<sub>6</sub>, 20 °C,  $\delta$ ) 3.02 (br s, CH<sub>2</sub>), 1.21 (br s, CH<sub>3</sub>). X = Br: IR (THF, cm<sup>-1</sup>) 2028 s, 2018 s, 2000 vs, 1990 vs, 1962 m (sh), 1932 m; <sup>11</sup>B NMR (THF, 20 °C,  $\delta$ ) 13.5 (br s); <sup>1</sup>H NMR (THF-*d*<sub>6</sub>, 20 °C,  $\delta$ ) 3.17 (br s, CH<sub>2</sub>), 1.32 (br s, CH<sub>3</sub>).

The neutral compounds themselves when dissolved in THF show the presence of these monoanions. IR spectrum of  $[HFe_4(CO)_{12}C]B(Cl)_2$  (THF, cm<sup>-1</sup>): 2028 vs, 2000 vs, 1980 m (sh), 1945 m. IR spectrum of  $[HFe_4(CO)_{12}C]BBR_2$  (THF, cm<sup>-1</sup>): 2030 vs, 2000 vs, 1945 m. <sup>11</sup>B NMR spectrum of  $[HFe_4(CO)_{12}C]B(Cl)_2$  (THF, 20 °C,  $\delta$ ): 29.9 (br s). <sup>11</sup>B NMR spectrum of  $[HFe_4(CO)_{12}C]BBR_2$  (THF, 20 °C,  $\delta$ ): 13.6 (br s).

**Synthesis of  $[HFe_4(CO)_{12}C]B(H)OH$ .**  $[HFe_4(CO)_{12}C]HBOH$  was formed in the reactions of  $[HFe_4(CO)_{12}C]BH(X)$  (X = Cl, Br; Br is much better than Cl) with THF after ca. 30 min at room temperature followed by removing THF under reduced pressure. Toluene was added and then removed under reduced pressure.

The residues were then soluble in hexane. Small crystals were obtained by fractional crystallization from the hexane solution at 0 °C. IR (hexane,  $\text{cm}^{-1}$ ): 3660 m (OH); 2510 w (BH); 2053 vs, 2034 s, 2023 s, 2000 m, 1992 m (sh) (CO).  $^{11}\text{B}$  NMR (hexane, 20 °C,  $\delta$ ): 26.3 (br d, fwhm 360 Hz,  $^1\text{H}$ ) 220 Hz;  $J_{\text{B-H}} = 140$  Hz).  $^1\text{H}$  NMR ( $\text{C}_6\text{D}_6$ , 20 °C,  $\delta$ ): 5.5 (br, BH), -26.72 (s, metal hydride). MS (EI,  $m/e$ ):  $\text{P}^+ = 602$  (-12 CO);  $^{56}\text{Fe}_4^{12}\text{C}_{13}^{16}\text{O}_{13}^{11}\text{B}^1\text{H}_3^+$ , 601.7054 (obsd), 601.7069 (calcd).  $^1\text{H}$  NMR spectrum of  $[\text{HFe}_4(\text{CO})_{12}\text{C}]\text{-BHBBr}$  ( $\text{THF-d}_8$ ,  $\delta$ ): 5.5 (br, BH), -26.38 (s, metal hydride).

**Crystallographic Studies for  $[\text{HFe}_4(\text{CO})_{12}\text{C}]\text{BHX}$ .** The crystallographic data for  $[\text{HFe}_4(\text{CO})_{12}\text{C}]\text{BXY}$  ( $\text{X} = \text{Y} = \text{H}$ ) have been published in the initial communication.<sup>16</sup> The data for  $\text{X} = \text{H}$ ,  $\text{Y} = \text{Cl}$ ,  $\text{Br}$  follow. Crystal data collection, and refinement parameters for  $\text{X} = \text{Cl}$ ,  $\text{Br}$  are collected in Table III. Crystals were mounted on glass fibers with epoxy cement. The unit-cell parameters were obtained from the least-squares fit of 25 reflections ( $20^\circ \leq 2\theta \leq 25^\circ$ ). Preliminary photographic evidence showed  $2/m$  Laue symmetry for both compounds. The systematic absences in diffraction data of both compounds established the  $2_1$  screw axis ( $0k0$ ,  $k = 2n + 1$ ). The centrosymmetric alternative,  $P2_1/m$ , was suggested by the  $E$  statistics of both, and this was confirmed by the chemically sensible results of refinement. Empirical absorption corrections were applied to both data sets (216  $\psi$ -scan reflections, pseudoellipsoid model,  $T_{\text{max}}/T_{\text{min}} = 1.585$  for  $\text{X} = \text{Cl}$  and 1.463 for  $\text{X} = \text{Br}$ ). The structure for  $\text{X} = \text{Cl}$  was solved by direct methods and that for  $\text{X} = \text{Br}$  by isomorphous

analogy to  $\text{X} = \text{Cl}$ . The remaining non-hydrogen atoms were located from subsequent difference Fourier syntheses. All non-hydrogen atoms were refined anisotropically. The metal-bridging hydride atoms in both were not located and were not included in the refinement. The Cl atom is disordered over two sites, Cl and Cl', in a 93:7 ratio. The atomic coordinates for the two compounds are given in Tables IV and V. All computer programs and the sources of the scattering factors are contained in the SHELXTL program library (version 5.1 by G. Sheldrick, Nicolet Corp., Madison, WI).

**Acknowledgment.** The support of the National Science Foundation is gratefully acknowledged. We thank Dr. B. Plashko for mass spectrometric measurements and Prof. S. G. Shore for suggesting the bonding model shown in Chart IIB. T.P.F. thanks the Department of Chemistry, University of Wisconsin—Madison, at which the calculations were carried out, for its hospitality while a Guggenheim Foundation Fellow.

**Supplementary Material Available:** Tables containing refined temperature factors and bond distances and angles for  $[\text{HFe}_4(\text{CO})_{12}\text{C}]\text{BHX}$  ( $\text{X} = \text{Cl}$ ,  $\text{Br}$ ) and a structural drawing of  $[\text{HFe}_4(\text{CO})_{12}\text{C}]\text{BHCl}$  (7 pages); tables of calculated and observed structure factors for  $[\text{HFe}_4(\text{CO})_{12}\text{C}]\text{BHX}$  ( $\text{X} = \text{Cl}$ ,  $\text{Br}$ ) (20 pages). Ordering information is given on any current masthead page.

## Synthesis of Large-Ring Keto Lactones by the Homogeneous and Polymer-Supported Palladium-Catalyzed Carbonylative Coupling of Esters Having Vinyl Triflate and Vinylstannane Termini

John K. Stille,<sup>†</sup> Heng Su, Dale H. Hill, Philippe Schneider, Masahide Tanaka, Donald L. Morrison, and Louis S. Hegedus\*

Department of Chemistry, Colorado State University, Fort Collins, Colorado 80523

Received October 16, 1990

Large-ring keto lactones having from 12 to 16 members were synthesized in fair yield by the palladium-catalyzed carbonylative coupling of long-chain esters having vinyl triflate and vinylstannane termini. A polystyrene-supported bis(diphenylphosphino)ferrocene ligand system was synthesized by the copolymerization of styrene, *p*-divinylbenzene, and bis(diphenylphosphino)vinylferrocene. Palladium catalysts supported on this polymer were more selective in these carbonylative cyclizations than were corresponding homogeneous catalyst systems.

### Introduction

There is a broad spectrum of naturally occurring medium- and large-ring compounds, many of which display some biological activity. These macrocycles are of varying complexity and contain a range of functional groups. They represent an important group of compounds, and their synthesis in relatively high yield represents important methodology. However, there are relatively few general methods for the generation of medium-sized and macrocyclic rings in high yield.<sup>1</sup> The reactions that yield carbocycles are often effected under severe enough reaction conditions that the range of compatible functional groups is limited, and when present, extensive protection/deprotection sequences are often necessary.

There are, however, a number of examples of the synthesis of macrocycles via transition-metal-mediated coupling reactions<sup>2-5</sup> that occur under relatively mild conditions and tolerate a range of functional groups. Rings

containing 9 to 27 members have been synthesized by this type of process.

The cross-coupling of an organic electrophile with an organometallic reagent is catalyzed by a number of group

(1) (a) Mandolini, L. *Intramolecular Reactions of Chain Molecules*. In *Advances in Physical Organic Chemistry*; Gold, V., Bethyl, D., Eds.; Academic Press: New York, 1986; Vol. 22. (b) Rossa, L.; Voegtli, F. *Synthesis of Medio- and Macrocyclic Compounds by High Dilution Principle Techniques*. *Top. Curr. Chem.* 1983, 113, 1. Winnik, M. A. *Chem. Rev.* 1981, 81, 491. Illuminati, G.; Mandolini, L. *Acc. Chem. Res.* 1981, 14, 95.

(2) Corey, E. J.; Kirst, H. A. *J. Am. Chem. Soc.* 1972, 94, 667.

(3) Ziegler, F. E.; Chakraborty, U. R.; Weisenfeld, R. B. *Tetrahedron* 1981, 37, 4035.

(4) (a) Trost, B. M.; Hane, J. T.; Metz, P. *Tetrahedron Lett.* 1986, 27, 5695. (b) Trost, B. M.; Warner, R. W. *J. Am. Chem. Soc.* 1983, 105, 5940.

(c) Trost, B. M.; Brickner, S. J. *J. Am. Chem. Soc.* 1983, 105, 568. (d) Trost, B. M.; Warner, R. W. *J. Am. Chem. Soc.* 1982, 104, 6112. (e) Trost, B. M.; Verhoeven, T. R. *J. Am. Chem. Soc.* 1980, 102, 4743. (f) Trost, B. M.; Verhoeven, T. R. *J. Am. Chem. Soc.* 1979, 101, 1595. (g) Trost, B. M.; Verhoeven, T. R. *Tetrahedron Lett.* 1978, 26, 2275. (h) Trost, B. M.; Verhoeven, T. R. *J. Am. Chem. Soc.* 1977, 99, 3867.

(5) (a) Takahashi, T.; Tsuji, J. *Kagaku (Kyoto)* 1987, 42, 356. (b) Takahashi, T.; Kataoka, H.; Tsuji, J. *J. Am. Chem. Soc.* 1983, 105, 147.

<sup>†</sup>Deceased on July 19, 1989.